

# CURRENT SOURCE INVERTER-FED AC MACHINE DRIVE SYSTEM

1 *DHRUPA PATEL Student of B.V.M Engineering collage, dhrupa1415@gmail.com*

2 *ASHISH R. PATEL Assistant Professor of B.V.M Engineering collage  
Electrical Department,*

**ABSTRACT** : *Current source inverter (CSI) is an attractive solution in high-power drives. The conventional gate turn-off thyristor (GTO) based CSI-fed ac machine drives suffer from drawbacks such as low-frequency torque pulsation, harmonic heating, and unstable operation at low-speed ranges. These drawbacks can be overcome by connecting a current-controlled voltage source inverter (VSI) across the motor terminal replacing the bulky ac capacitors. The VSI provides the harmonic currents, which results in sinusoidal motor voltage and current even with the CSI switching at fundamental frequency. This paper presents new five-level current-source inverters (CSIs). A current source inverter (CSI) requires a capacitor filter for the commutation of switching device as well as for attenuating switching harmonics. Hence, the CSI-fed ac machine has a second-order system in the continuous time domain. The proposed strategy features the following: 1) an on-line operated PWM inverter, using instantaneous output capacitor voltage control based on space-vector modulation and 2) an additional inverter modulation index control loop, ensuring constant inverter modulation index and minimum dc-link current operation. The resulting additional advantages include the following: 1) fixed and reduced motor voltage distortion; 2) minimized dc-bus inductor losses; 3) minimized switch conduction losses; and 4) elimination of motor circuit resonances. Experimental results based on a digital signal processor implementation are given.*

**Index Terms**— *AC drive, pulsewidth modulation current-source rectifier/inverter,*

## I. INTRODUCTION

CURRENT-SOURCE INVERTER (CSI) has traditionally been adopted for relatively high-power applications, where a source of constant dc input current is readily available, such as in the medium voltage ac drive with a controlled rectifier [1] and superconducting magnetic energy storage [2]. The common reasons stated for using a CSI in these applications are its inherent bidirectional operation, short-circuit protection, and a smoother set of output voltage waveforms suitable for driving ac motors without causing excessive insulation stress and induced shaft voltage [3]. Surely, a CSI has its disadvantages too like its generally slower dynamic response and bulky overall size caused mainly by the inclusion of a large smoothing inductor at its dc source end. However, depending on the particular applications under consideration, its advantages can at times outweigh its disadvantages, hence rendering it as a suitable choice for these applications.

The scope of application of CSI has continued to grow over the years with a few recent examples found in [4]–[5], covering both high- and low-power usages. The latter is interesting, since it demonstrates that CSI has started to penetrate into the low-power range with [5] showing how it can be configured as a solar-grid-connected inverter and a split single-phase residential supply, respectively. More application examples are likely to surface in the near coming future, particularly after the invention of reverse-blocking active switches has made the construction of a CSI a more convenient task. Because of this same

reason, research on CSI topological development is active too with some researchers aiming to combine merits of a voltage-source inverter (VSI) and a CSI to form a hybrid topology with improved dynamic current response, lower switching loss, and better waveform quality than when only a single VSI or CSI is used [6]. Yet, other researchers are exploring the development of multilevel (usually five level) CSI, previously shown to have advantages similar to those inherited by a multilevel VSI like a better output waveform quality, lower electromagnetic interference, and lower device current stress to name only a few [7].

Indeed, the development of multilevel CSI has progressed reasonably smoothly with a few feasible five-level topologies reported in the literature and shown in Fig.1 Looking first at the topology shown in Fig.1(a), it consists of two CSI bridges tied together by inductances  $L_1$  and  $L_2$  and powered by an input current source [8]. Although it can be viewed as a cost-saving option since only a single-input source is needed, some mechanisms (either through modulation or some explicit hardware inclusion) for continuously maintaining the relevant current ratio between the two bridges are needed, which unfortunately might complicate the system and its reliability. As a second option, the direct paralleling of two independent CSI bridges shown in Fig.1(b) appears to be a more straight forward topology [9], but its realization is definitely more costly, since two independent current sources are needed.

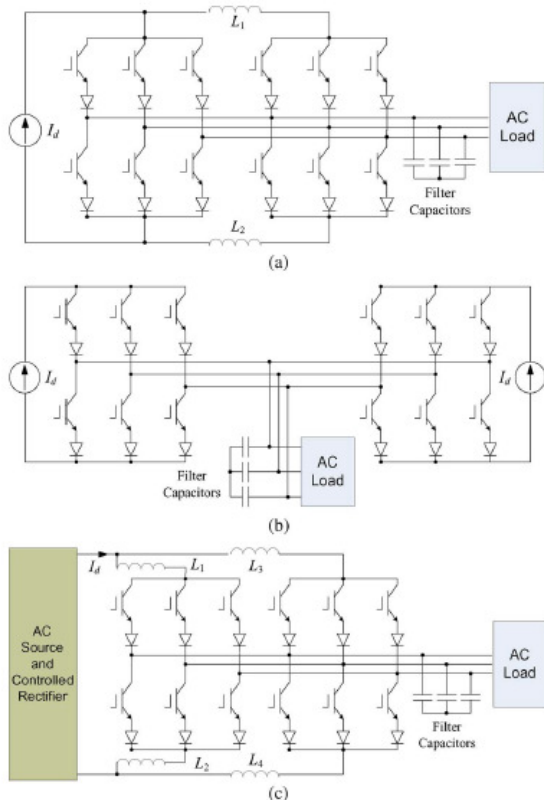


Fig.1 Three-phase schematics of five-level CSIs reported in (a) [10], [11], (b) [12], [13], and (c) [14].

Indeed, these two earlier described topologies can produce the required five-level ac current switching, but their overall setup cost (components and space) can be high, particularly when the large dc inductors connected in series with the voltage sources to form the input current sources are taken into consideration. These dc source inductors are usually larger in size and higher in current rating [e.g., likely to be higher than  $L_1$  and  $L_2$  in Fig.1(a)], since they have to sustain a higher and smoother current for powering the two CSI bridges. Therefore, an attempt to remove them from the input source is pursued in [10] to give the third feasible CSI circuit shown in Fig.1(c). As shown in the figure, no common dc source inductor is used. Instead, the current is smoothed by the separate smaller inductor pairs found in each bridge ( $L_1$  and  $L_2$  to bridge 1 and  $L_3$  and  $L_4$  to bridge 2), which to a favorable extent is deemed as a more economical method of filtering. The input source can now be obtained by simply rectifying the ac mains, but in spite of that, the problem of balancing the dc inductive current among the two bridges still has to be resolved and is generally solved by control modifications or adding relevant hardware.

In common, the topologies shown in Fig.1 are therefore summarized to lack control flexibility in the sense that only voltage-boost (or current-buck) operation is supported. Therefore, they would have difficulties maintaining a constant output voltage (or

current) if the input voltage rises too far upward or supporting low-voltage (or high current) load operation if given a constrained constant input source. To overcome this limitation, a number of buck-boost CSI variations have been developed over the years with [11] presenting two possible examples. Although proven to function well, existing buck-boost CSIs are developed using only a single three level bridge with their extension to higher level inverters left unexplored. Of course, various reasons can be stated for the lack of activities in that area of research, but technically, the likely hindrances are the significant increases in component count (and hence cost), control complexity, and difficulty in balancing the dc inductive currents even when only two CSI bridges are tied together.

## II. CSI AC MACHINE DRIVE

Traditionally, current source inverter (CSI) had been used for the high power drives due to its ruggedness to over current/short circuit and low  $dv/dt$  stress over the stator windings of the electric machine [12], [13]. Recently, because of aforementioned inherent advantages of CSI, effort has been increased to drive the ac system with CSI in high power drives such as wind power generation and hybrid electric vehicles [14]–[15].

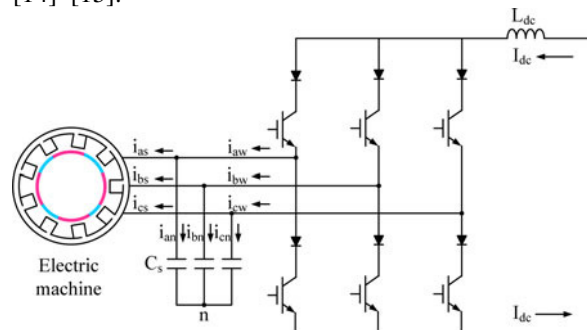


Fig.2 Block diagram of IGBT-based CSI-fed an electric machine

There was a comparative study with consideration on the selection of power semiconductors for CSI [16]. In this paper, the insulated gate bipolar transistor (IGBT) is adopted to increase the switching frequency more than 1 kHz even in multi-MW drive systems because the cost and size of passive components can be reduced as the switching frequency is increased [16]. A CSI-fed electric machine can be depicted as shown in Fig.2 A three-phase filter capacitor  $C_s$  is required for the commutation of switching devices and for filtering out the current harmonics flowing into the electric machine.

Due to this filter capacitor, the CSI-fed drive system has an inherent issue with LC resonance. The filter capacitor forms an LC filter along with the stator inductance of the electric machine and step current input from the output of the CSI can incur oscillation

in the phase currents. Because a passive damping method with a physical resistor results in excessive energy losses, there were many studies to dampen the LC resonance with active control strategies. In order to reduce the resonance, there were several approaches which are the virtual resistor damping method [17], an active damping method using inductor current feedback control [18], a feed forward compensation method from the LC filter model [19], a compensator design method [20], and a hybrid type method with a virtual resistor and a compensator [21] for the open-loop control. On the other hand, for the closed-loop control, the multiloop controller can generally be used to control the output with a higher order plant such as the CSI-fed drive system employing an LC filter [22]. There were studies about the multiloop controller for the voltage source inverter (VSI) with an LCL filter and CSI with an LC filter [22], [23]. In these studies, the proportional and resonant controller was used to attenuate the resonance instead of the PI controller in the synchronous reference frame.

### III. SYSTEM DESCRIPTION

The CSI-fed ac machine drive system in synchronous reference frame can be modelled as (1)–(3). The voltage and current equation of a non-salient ac machine is employed for modelling such as an induction machine or a surface mounted permanent magnet synchronous machine (SMPMSM) or a synchronous reluctance machine

$$\begin{bmatrix} i_{dw}^e \\ i_{qw}^e \end{bmatrix} = \begin{bmatrix} i_{ds}^e \\ i_{qs}^e \end{bmatrix} + \begin{bmatrix} i_{dn}^e \\ i_{qn}^e \end{bmatrix} \quad (1)$$

$$\begin{bmatrix} i_{dn}^e \\ i_{qn}^e \end{bmatrix} = \begin{bmatrix} pC_s & -\omega_e C_s \\ \omega_e C_s & pC_s \end{bmatrix} \begin{bmatrix} v_{ds}^e \\ v_{qs}^e \end{bmatrix} \quad (2)$$

$$\begin{bmatrix} v_{ds}^e \\ v_{qs}^e \end{bmatrix} = \begin{bmatrix} R_s + pL_s & -\omega_e L_s \\ \omega_e L_s & R_s + pL_s \end{bmatrix} \begin{bmatrix} i_{ds}^e \\ i_{qs}^e \end{bmatrix} + \begin{bmatrix} e_{ds}^e \\ e_{qs}^e \end{bmatrix} \quad (3)$$

Where  $i_{dqw}^e$  denotes d- and q-axes output current of a CSI,  $i_{dqs}^e$  denotes d- and axes stator current of an ac machine,  $i_{dqn}^e$  denotes d- and q-axes current of a filter capacitor,  $v_{dqs}^e$  denotes d and q-axes voltage of a filter capacitor,  $R_s$  denotes a stator resistance of an ac machine,  $L_s$  denotes a synchronous inductance of an ac machine,  $\omega_e$  denotes a synchronous angular speed of an ac machine,  $e_{dqs}^e$  denotes a back-emf voltage of an ac machine, and  $p$  denotes a differential operator. From those equations, the equivalent circuit can be derived as shown in Fig.3

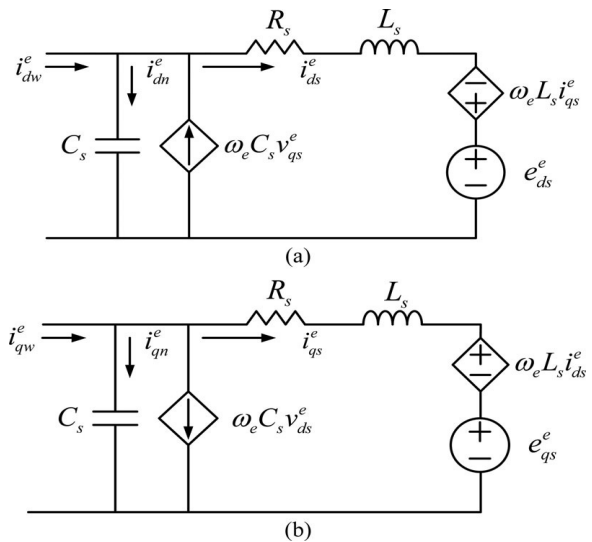


Fig.3 Equivalent circuit of CSI including the ac system and capacitor filter in the synchronous reference frame. (a) d-axis equivalent circuit. (b) q-axis equivalent circuit.

### IV. VSI/CSI AC MACHINE DRIVE (MERITS/DEMERITS)

Voltage source inverter (VSI) fed induction motor drive is an attractive solution for low-power applications because of the availability of fast switching devices like insulated gate bipolar transistor (IGBT) and MOSFET. But for medium and high-power applications, VSI cannot switch as fast as in the case of the low-power counterpart due to increased switching loss. Furthermore, for medium-voltage applications, the devices of required voltage rating for two-level VSI are not readily available. Multilevel VSIs [24] are used in medium-voltage applications as the device voltage stress decreases with the increase in the number of levels of multilevel VSIs. VSI-fed induction motor drives have certain drawbacks as follows:

- 1) The voltage overshoots caused by the long cable connected between the converter and the motor are detrimental to motor insulation [25].
- 2) Additional losses in the motor caused by the high-frequency current ripple.
- 3) Electromagnetic emission caused by the high dV/dt in the cable.
- 4) Common-mode voltage and bearing current in the motor.

Current source inverter (CSI) fed induction motor drive is an attractive solution for high-power applications due to its inbuilt shoot through protection and regenerative capability. CSIs are considered for drive applications and as an interface of variable-speed wind generators with fixed-frequency grid [26],[27]. Due to a large dc link inductor connected at the output of the phase-controlled rectifier, the dynamic response of the torque of the motor is poor compared to that of VSI-fed induction motor drive. This drive is suitable for fan and pump type of load, where dynamic response

of the torque is not of major concern. Fig.4 (a) shows the schematic diagram of the conventional CSI-fed induction motor drive with output capacitor. With self-commutating devices like gate turn-off thyristor (GTO) in the CSI, pulse width modulation (PWM) of CSI output current can be done to get better quality motor current and voltage [28]. But for large induction motor drives, the switching frequency is low to minimize switching losses. Bulky ac capacitors have to be employed at the motor terminal to reduce the voltage spikes due to switching of the currents. These capacitors form two modes of resonance with motor magnetizing inductance and leakage inductance. The resonating modes are clearly explained in [29] and selective harmonic elimination techniques are proposed to avoid them. But it is not possible to completely avoid resonance at low values of fundamental frequency.

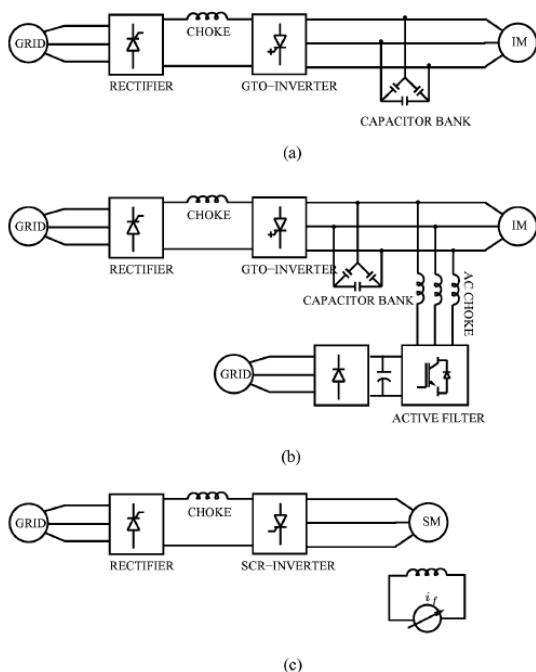


Fig.4 Functional block diagrams of existing configurations of CSI-fed ac motor drives. (a) Functional block diagram of conventional CSI-fed induction motor drive. (b) Functional block diagram of CSI-fed induction motor drive with an active filter connected across the motor terminal. (c) Functional block diagram of LCI-fed synchronous motor drive.

A CSI-based ac induction machine drive with the following features: 1) the motor voltage, rather than the motor current, is regulated on-line by using a feedback control technique and 2) the dc-link current is regulated to the minimum value required to keep the inverter modulation index constant and independent of the speed reference and load torque. Furthermore, other features include the following:

1) the entire control strategy is implemented in a digital signal processor (DSP) system, based on the

TMS320C30 chip; 2) the overall speed control strategy is based on a constant voltage/frequency (V/f) scalar control technique; 3) both rectifier and inverter stages are PWM and space-vector modulated. The above features lead to the following advantages over conventional CSI motor drive implementations: 1) the gating signals are directly generated by the space vector digital modulator (extra circuitry is only necessary to ensure overlaps); 2) the potential resonances are eliminated due to the feedback-based voltage controller; 3) the stresses on power switches and the overall losses are always minimum due to the minimum dc-link current operation; and 4) due to the constant inverter modulation index operation, the motor voltage harmonic distortion is constant, which minimizes the induction motor losses and allows an accurate output filter design. These features make the CSI drive an interesting alternative to VSI-based drives operating at similar switching frequency, when the requested fundamental reactive power could be disregarded with respect to output power.

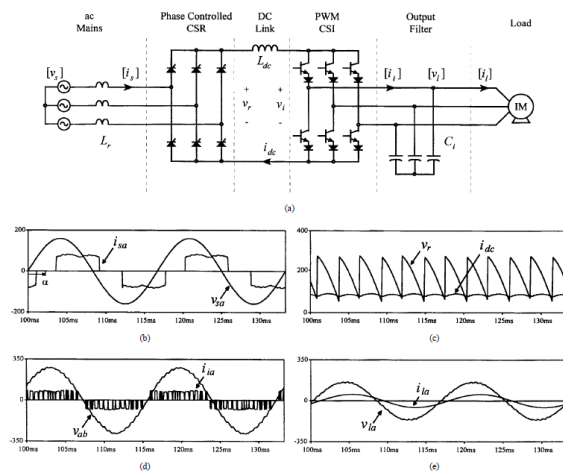


Fig.5 AC drive CSI based on a phase-controlled front-end rectifier (50% nominal load and 50-Hz output). (a) Power topology. (b) Supply phase voltage ( $v_{sa}$ ) and supply line current (15 .  $i_{sa}$ ). (c) DC rectifier voltage ( $v_r$ ) and dc-link current (15 .  $i_{dc}$ ). (d) CSI line current ( $i_{ia}$ ) and load line voltage ( $v_{ab}$ ). (e) Load phase voltage ( $v_{la}$ ) and load line current (15 .  $i_{la}$ ).

A complete comparison with standard CSI-based ac drives is also presented. Key performance indices, such as harmonic distortion (THD), PF, and time response are evaluated and tabulated for both the standard and the proposed schemes. experimental results are given for a 2-kVA induction motor drive.

#### V. STANDARD CSI-BASED AC DRIVES

In this paper, drive classification is based on the structure of the front-end power converter, which could be either a phase-controlled thyristor rectifier or a PWM current-source rectifier.

**A. Phase-Controlled Front-End Rectifiers**

These drives use a front-end rectifier based on thyristor-type power switches (Fig.5), which can be operated with either variable or fixed dc-link current. The performance of the drive converter depends on this last feature.

1) Variable DC-Link Current Scheme The CSI is operated with a fixed pattern, which is usually optimized in terms of harmonic spectrum and switching frequency. Thus, the load voltage harmonic distortion (THDV) is minimum and constant (Table I). However, the dc-link current must be adjusted through transient changes in firing angle to meet the requirements of the load. The dc voltage, on the other hand, is practically constant and independent of the load torque.

This last feature leads to a constant input current displacement factor and, thereby, a constant overall PF (Table I). Also, since the dc-link current tracks the output current, the dc-bus and switch conduction losses are kept to a minimum. Usually, the dc-link inductor is designed to have an acceptable current ripple (5%). In order to achieve this value and due to the low-order harmonics produced by the thyristor rectifier (sixth, 12th, etc.), the size of the dc inductor becomes quite bulky. This results in a slow system transient response. Also, the supply current has a high distortion factor (THDi = 142%) due to the low-order harmonics (fifth, seventh, etc.) injected by the thyristor rectifier. Fig.5 shows typical waveforms of the converter. The rectifier phase angle ( $\alpha$ ) is only adjusted during transient conditions occurring under load speed and torque variations.

2) Fixed DC-Link Current Scheme Unlike the above control scheme, the CSI is operated with a PWM pattern, which varies as a function of the CSI modulation index. Therefore, the load voltage harmonic distortion (THDV) is variable and depends upon the speed and load torque (Table I). Since the dc-link current is fixed, the different load power requirements are obtained by varying the dc-link voltage. To achieve this, the input PF becomes variable and closes to zero for light loads. Contrary to the variable dc-link current scheme, the dc-bus and switch conduction losses are always maximum, due to the fact that the dc-link current is always maximum (Table I). Although the dc-link inductor size is as big as the one used in the above scheme, the dynamic response of the load current is improved, due to the variable PWM pattern approach with time responses to modulation index changes of the order of a sampling period. This scheme also presents a high supply current harmonic distortion, due to the thyristor rectifier operation (Table I). Typical waveforms shown in Fig.5 are also applicable in this case; however, in this mode of operation, the rectifier phase angle ( $\alpha$ ) is continuously adjusted to maintain a

constant dc-link current, regardless of the load speed and torque.

**B. PWM Front-End Rectifiers**

Unlike phase-controlled rectifier topologies, this topology uses a PWM rectifier (Fig.6). This allows a reduction in the harmonics injected into the ac supply. The rectifier is operated with a fixed dc-link current. Fig.6 shows typical waveforms of the converter. The PWM pattern is adjusted on a continuous basis to keep a constant dc-link current. In contrast to topologies based on thyristor front-end rectifiers, the overall drive input PF is always greater than 0.95, and the total input current harmonic distortion, which depends on the sampling frequency, is typically lower than 10% (Table I). Also, since the output inverter is PWM modulated, the system has time responses close to the sampling period. However, the dc-bus losses and switch conduction losses are maximum, since the dc-link current is always equal to its maximum value, regardless of the load speed and torque.

**VI. PROPOSED AC DRIVE SYSTEM DESCRIPTION**

**A. Power Circuit**

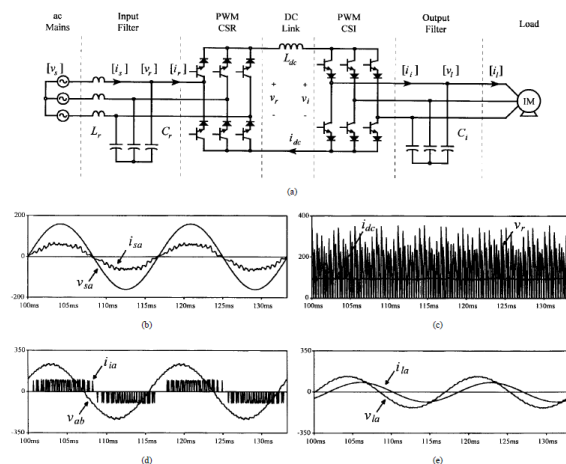


Fig.6 AC drive CSI based on a PWM front-end rectifier (50% nominal load and 50-Hz output). (a) Power topology. (b) Supply phase voltage ( $v_{sa}$ ) and supply line current ( $15 \cdot i_{sa}$ ). (c) DC rectifier voltage ( $v_r$ ) and dc-link current ( $15 \cdot i_{dc}$ ). (d) CSI line current ( $i_{ia}$ ) and load line voltage ( $v_{ab}$ ). (e) Load phase voltage ( $v_{la}$ ) and load line current ( $15 \cdot i_{la}$ ).

The complete power circuit (Fig.6) belongs to the second category described above, therefore, it is composed of a three phase PWM rectifier, a dc-link reactor, and a three-phase PWM CSI.

**B. Control System Structure**

The general control diagram of the proposed CSI-based ac drive is shown in Fig.7 Unlike the fixed dc-link current scheme, this scheme varies the dc-link current, in order to keep the CSI modulation index

constant in steady state. The global control strategy is composed of two main control loops.

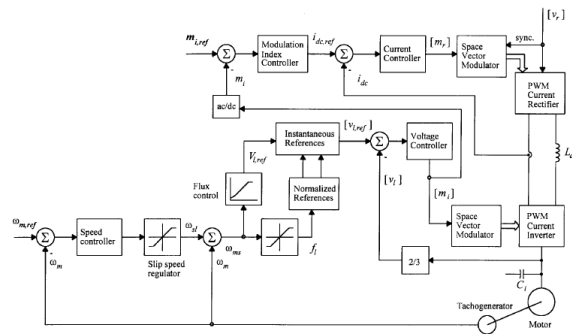


Fig.7 Control scheme of the proposed ac drive CSI incorporating modulation index control for reduced losses (motor control uses the V=f scheme).

The first control loop is the motor speed control ( $\omega_m$ ) based on a slip speed regulator, which sets the slip speed reference ( $\omega_{sl}$ ). The synchronous speed ( $\omega_{ms}$ ), obtained by adding the actual speed and the slip speed, determines the inverter frequency ( $f_i$ ). The motor voltage reference signal is ( $V_{l,ref}$ ) constructed from the frequency using a function generator, which ensures a nearly constant flux operation. Finally, the voltage controller and the space-vector modulator produce the switching pattern ( $s_i$ ) based on the difference between the sine voltage reference waveforms ( $v_{l,ref}$ ) and the sampled load voltage waveforms ( $v_l$ ). This feedback scheme ensures that the CSI gating pattern is modified on-line, so as to force the output voltage  $v_i$  to track the reference  $v_{l,ref}$  thereby resulting in a fast dynamic response, with rise times in the range of the sampling period ( $t_{sample}$ ) of the space-vector technique. Analysis and design guidelines of this inner motor voltage loop are given in [30].

The second control loop is the PWM CSI modulation index loop ( $m_i$ ). The main function of this slower loop is to set online the dc-link current reference ( $i_{dc,ref}$ ) in such a way that the steady-state PWM CSI modulation index remains equal to the reference ( $m_{i,ref}$ ). The next section demonstrates theoretically that, by properly adjusting the dc-link current, the modulation index of the CSI can be effectively regulated.

#### VII. THE MODULATION INDEX CONTROL LOOP

This loop is designed to be slower than the dc-link current and the motor voltage loops. This feature allows one to consider that the actual dc current and actual motor voltages are equal to their respective references when analyzing the dynamic of the modulation index loop. Thus, the dc-link stage can be modeled by a pure current source with a value equal

to the reference ( $i_{dc,ref}$ ) and the CSI dc-bus voltage approximated by

$$v_i = m_{ia} v_{la,ref} + m_{ib} v_{lb,ref} + m_{ic} v_{lc,ref} \quad (4)$$

where,  $m_{ia}$ ,  $m_{ib}$ , and  $m_{ic}$  are the time-average modulating signals generated by the space-vector modulation technique  $v_{la,ref}$ ,  $v_{lb,ref}$  and  $v_{lc,ref}$ , are the motor phase voltage references. Since the motor voltages references and the modulating signals are sinusoidal quantities, they can be represented by

$$\begin{bmatrix} m_{ia} \\ m_{ib} \\ m_{ic} \end{bmatrix} = m_i \begin{bmatrix} \sin(\omega t) \\ \sin(\omega t - 120^\circ) \\ \sin(\omega t - 240^\circ) \end{bmatrix} \quad (5)$$

and

$$\begin{bmatrix} v_{la} \\ v_{lb} \\ v_{lc} \end{bmatrix} = \sqrt{2} \frac{V_l}{\sqrt{3}} \begin{bmatrix} \sin(\omega t - \Psi) \\ \sin(\omega t - 120 - \Psi) \\ \sin(\omega t - 240 - \Psi) \end{bmatrix} \quad (6)$$

where  $m_i$  is the CSI modulation index,  $V_l$  is the motor line rms voltage,  $\omega$  the motor voltage frequency, and  $\Psi$  is an angle which depends upon the operating conditions and system parameters. Using (5) and (6), the CSI dc-bus voltage (4) can be rewritten as

$$v_i = \sqrt{\frac{3}{2}} m_i v_l \cos(\Psi) \quad (7)$$

If the CSI and the output filter are considered lossless, the CSI instantaneous power balance indicates that

$$v_i i_{dc,ref} = \sqrt{\frac{3}{2}} m_i i_{dc,ref} V_l \cos(\Psi) = p_l \quad (8)$$

where  $p_l$  is the load power. Equation (8) shows that, in order to control the load power, either the dc-link current ( $i_{dc,ref}$ ) or the CSI modulation index ( $m_i$ ) can be adjusted. In this paper, a combination of the two quantities is used in a cascade strategy (Fig.6). Transient changes in the load are accommodated by adjusting the CSI modulation index through the inner motor voltage loop. In addition, the slower CSI modulation index outer loop adjusts the dc-link current to maintain the CSI modulation index to a high value under steady-state conditions. It can also be seen from (8) that, by maximizing the modulation index, the dc-link current is minimized. These features and their effect are evaluated experimentally in the next section.

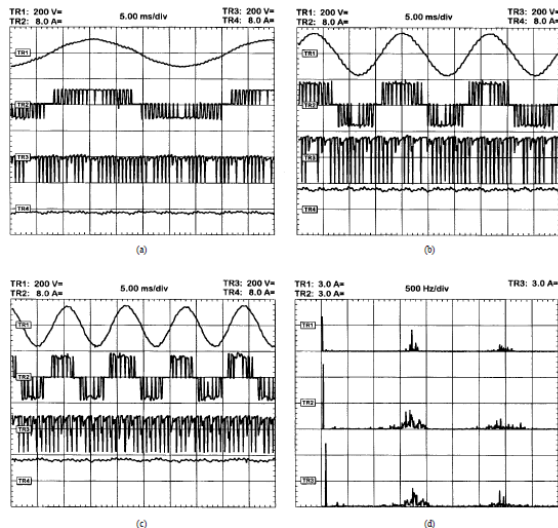


Fig. 8. Experimental waveforms for the proposed CSI-based ac drive. (a) 30-Hz operation. (b) 60-Hz operation. (c) 90-Hz operation. (TR1: motor line voltage ( $v_{ab}$ ); TR2: CSI line current ( $i_{ia}$ ); TR3: CSI dc-bus voltage ( $v_i$ ); TR4: dc-link current ( $i_{dc}$ .) (d) CSI line current spectrum ( $i_{ia}$ ). (TR1: 30-Hz operation; TR2: 60-Hz operation; TR3: 90-Hz operation.)

It should be noted that a high modulation index set point under steady-state conditions ( $M_i$  near 1.0) is desired, in order to minimize the dc-link current and to obtain low harmonic distortion waveforms on the load side. However, a lower modulation index would provide a wider operating range before the CSI modulator goes into saturation ( $M_i > 1.0$ ) under transient conditions. When the modulation index reaches its maximum, the slower acting modulation index controller will increase the dc-link current to meet the load requirements. The converter then operates as a standard fixed dc-bus current CSI drive. This is an intrinsic limitation of the proposed control strategy. Simulation and experimental studies have shown that a modulation index equal to 0.8 provides a good compromise between steady-state and transient operation requirements. Specifically, this set point provides a 20% transient current increase before the CSI modulator goes into saturation.

The linearization of (8) gives

$$\Delta m_i = -\frac{M_i}{I_{dc,ref}} \Delta I_{dc,ref} + \frac{M_i}{P_i} \Delta p_l \quad (9)$$

where  $M_i$ ,  $P_i$  and  $I_{dc,ref}$  are the values of  $m_i$ ,  $p_l$  and  $i_{dc,ref}$  at the operating point, and  $\Delta m_i$ ,  $\Delta p_l$ , and  $\Delta I_{dc,ref}$  are the small deviations of  $m_i$ ,  $p_l$ , and  $i_{dc,ref}$  around the operating point. Note that  $\Delta p_l$  becomes a perturbation and  $M_i$ ,  $P_i$  and  $i_{dc,ref}$  are obtained from (8) evaluated at the operating point. The small-signal model (9) shows an inverse relation between the dc-link current and the CSI modulation

index. Therefore, a linear controller with a negative gain can provide the necessary compensation to obtain a stable closed loop. In this paper, a proportional integral (PI) controller ten times slower than the output voltage loop is implemented.

#### VIII. ACKNOWLEDGEMENT

This paper gives fundamental details of CSI fed AC machine drive system. This paper is prepared from various references. The author would like to acknowledge all the references, whose detail directly or indirectly consider for this study paper.

#### IX. CONCLUSION

A CSI-based ac induction motor drive topology with a supplemental CSI modulation index control loop has been proposed. The control strategy allows the operation of the inverter at constant modulation index in steady state, regardless of the load speed and torque. The strategy achieves this goal by minimizing the steady-state dc-link current. In addition to the inherent advantages of the CS topology (short-circuit protection, low output, and regeneration capabilities), the proposed control scheme adds the following advantages: 1) fixed and reduced motor voltage distortion; 2) minimized dc-bus and switch conduction losses; and 3) elimination of motor circuit resonances through instantaneous output voltage control. Experimental results based on a DSP implementation confirm these features.

#### REFERENCES

- [1] J. Rodriguez, J. Pontt, N. Becker, and A. Weinstein, "Regenerative drives in the megawatt range for high-performance downhill belt conveyors," *IEEE Trans. Ind. Appl.*, vol. 38, no. 1, pp. 203–210, Jan./Feb. 2002.
- [2] Z. C. Zhang and B. T. Ooi, "Multimodular current-source SPWM converters for a superconducting magnetic energy storage system," *IEEE Trans. Power Electron.*, vol. 8, no. 3, pp. 250–256, Jul. 1993.
- [3] V. D. Colli, P. Cancelliere, F. Marignetti, and R. Di Stefano, "Influence of voltage and current source inverters on low-power induction motors," *Proc. Inst. Elect. Eng.—Elect. Power Appl.*, vol. 152, no. 5, pp. 1311–1320, Sep. 2005.
- [4] E. P. Wiechmann, P. Aqueveque, R. Burgos, and J. Rodriguez, "On the efficiency of voltage source and current source inverters for highpower drives," *IEEE Trans. Ind. Electron.*, vol. 55, no. 4, pp. 1771–1782, Apr. 2008.
- [5] N. Stretch and M. Kazerani, "A stand-alone, split-phase current-sourced inverter with novel energy storage," *IEEE Trans. Power Electron.*, vol. 23, no. 6, pp. 2766–2774, Nov. 2008.
- [6] A. M. Trzynadlowski, N. Patriciu, F. Blaabjerg, and J. K. Pedersen, "A hybrid, current-source/voltage-source power inverter circuit," *IEEE*

- Trans. Power Electron., vol. 16, no. 6, pp. 866–871, Nov. 2001.
- [7] M. D. Manjrekar, P. K. Steimer, and T. A. Lipo, “Hybrid multilevel power conversion system: a competitive solution for high-power applications,” *IEEE Trans. Ind. Appl.*, vol. 36, no. 3, pp. 834–841, May/June 2000.
- [8] F. L. M. Antunes, H. A. C. Braga, and I. Barbi, “Application of a generalized current multilevel cell to current-source inverters,” *IEEE Trans. Ind. Electron.*, vol. 46, no. 1, pp. 31–38, Feb. 1999.
- [9] S. Kwak and H. A. Toliyat, “Multilevel converter topology using two types of current-source inverters,” *IEEE Trans. Ind. Appl.*, vol. 42, no. 6, pp. 1558–1564, Nov./Dec. 2006.
- [10] J. R. Espinoza, L. A. Moran, and J. I. Guzman, “Multi-level three-phase current source inverter based AC drive for high performance applications,” in *Proc. IEEE Power Electron. Spec. Conf.*, 2005, pp. 2553–2559.
- [11] P. C. Loh, P. C. Tan, F. Blaabjerg, and T. K. Lee, “Topological development and operational analysis of buck–boost current source inverters for energy conversion applications,” in *Proc. IEEE Power Electron. Spec. Conf.*, 2006, pp. 1033–1038.
- [12] M. Salo and H. Tuusa, “Vector-controlled PWM current-source-inverter-fed induction motor drive with a new stator current control method,” *IEEE Trans. Ind. Electron.*, vol. 52, no. 2, pp. 523–531, Apr. 2005.
- [13] Z. Wang, B. Wu, D. Xu, and N. R. Zargari, “Hybrid PWM for high-power current-source inverter-fed drives with low switching frequency,” *IEEE Trans. Power Electron.*, vol. 26, no. 6, pp. 1754–1764, Jun. 2011.
- [14] J. Dao, D. Xu, and B. Wu, “A novel control scheme for current-source converter-based PMSG wind energy conversion systems,” *IEEE Trans. Power Electron.*, vol. 24, no. 4, pp. 963–972, Apr. 2009.
- [15] Z. Wu and G. J. Su, “High-performance permanent magnet machine drive for electric vehicle applications using a current source inverter,” in *Proc. Conf. IEEE Ind. Electron.*, Nov. 2008, pp. 2812–2817.
- [16] H. Bilgin and M. Ermis, “Design and implementation of a current-source converter for use in industry applications of D-STATCOM,” *IEEE Trans. Power Electron.*, vol. 25, no. 8, pp. 1943–1957, Aug. 2010.
- [17] J. C. Wiseman and B. Wu, “Active damping control of a high-power PWM current-source rectifier for line-current THD reduction,” *IEEE Trans. Ind. Electron.*, vol. 52, no. 3, pp. 758–764, Jun. 2005.
- [18] F. Liu, B. Wu, N. R. Zargari, and M. Pande, “An active damping method using inductor-current feedback control for high-power PWM current source rectifier,” *IEEE Trans. Power Electron.*, vol. 26, no. 9, pp. 2580–2587, Sep. 2011.
- [19] M. Salo and H. Tuusa, “A vector controlled current-source PWM rectifier with a novel current damping method,” *IEEE Trans. Power Electron.*, vol. 15, no. 3, pp. 464–470, May 2000.
- [20] Y. Neba, “A simple method for suppression of resonance oscillation in PWM current source converter,” *IEEE Trans. Power Electron.*, vol. 20, no. 1, pp. 132–139, Jan. 2005.
- [21] Y. W. Li, B. Wu, N. R. Zargari, J. C. Wiseman, and D. Xu, “Damping of PWM current-source rectifier using a hybrid combination approach,” *IEEE Trans. Power Electron.*, vol. 22, no. 4, pp. 132–139, Jul. 2007.
- [22] P. C. Loh and D. G. Holmes, “Analysis of multiloop control strategies for LC/CL/LCL-filtered voltage-source and current-source inverters,” *IEEE Trans. Ind. Appl.*, vol. 41, no. 2, pp. 644–654, Mar./Apr. 2005.
- [23] Y. W. Li, “Control and resonance damping of voltage-source and current source converters with LC filters,” *IEEE Trans. Ind. Electron.*, vol. 56, no. 5, pp. 1511–1521, May 2009.
- [24] A. R. Beig, “Application of three level voltage source inverters to voltage fed and current fed high power induction motor drives,” Ph.D. dissertation, Dept. Electr. Eng., Ind. Inst. Sci. (IISc), Bengaluru, India, Apr. 2004.
- [25] J. C. G. Wheeler, “Effects of converter pulses on the electrical insulation in low and medium voltage motors,” *IEEE Electr. Insul. Mag.*, vol. 21, no. 2, pp. 22–29, Mar./Apr. 2005.
- [26] P. Tenca, A. A. Rockhill, T. A. Lipo, and P. Tricoli, “Current source topology for wind turbines with decreased mains current harmonics, further reducible via functional minimization,” *IEEE Trans. Power Electron.*, vol. 23, no. 3, pp. 1143–1155, May 2008.
- [27] B. Wu, *High Power Converters and AC Drives*. Piscataway, NJ/New York: IEEE Press/Wiley, 2006.
- [28] P. M. Espelage, L. M. Nowak, and L. H. Walker, “Symmetrical GTO current source inverter for wide speed range control of 2300 to 4160 Volt, 350 to 7000 Hp, induction motors,” in *Proc. IEEE Ind. Appl. Soc. Annu. Meeting*, Pittsburgh, PA, Oct. 27, 1988, vol. 1, pp. 302–307.
- [29] B. Wu, S. B. Dewan, and G. R. Slemon, “PWM CSI inverter for induction motor drives,” *IEEE Trans. Ind. Appl.*, vol. 28, no. 1, pp. 64–71, Jan./Feb. 1992.
- [30] S. Kwak and H. A. Toliyat, “A hybrid solution for load-commutated inverter-fed induction motor drives,” *IEEE Trans. Ind. Appl.*, vol. 41, no. 1, pp. 83–90, Jan./Feb. 2005.